Comprehensive multi-omics analysis identifies cancer subtypes and prognostic signatures of hepatitis B virus–associated hepatocellular carcinoma

Rui Wang[1,2], Bo Ren[1,2], Xijie Zhang[1,2], Bo Liu[1,2], Wence Zhou[1,2,3]

[1] The Second Clinical Medical School, Lanzhou University, Lanzhou, China.

[2] Department of General Surgery, The Second Hospital of Lanzhou University, Lanzhou, China.

[3] Gansu Province Hepatobiliary Pancreatic Disease Precision Diagnosis and Treatment Engineering Research Center, Lanzhou, China.

Corresponding author:

Wence Zhou, The Second Clinical Medical School, Lanzhou University, Lanzhou, China. Department of General Surgery, The Second Hospital of Lanzhou University, Lanzhou, China. Gansu Province Hepatobiliary Pancreatic Disease Precision Diagnosis and Treatment Engineering Research Center, Lanzhou, China. Email: zhouwc129@163.com.

Supplementary Table 1. Differences in clinical characteristics between different HBV-HCC cancer subtypes.

Clinical characteristic	Level	CS1 (n=72)	CS2 (n=27)	*p*-value
Futime (Days) (median [IQR])	/	699.50 [531.50, 1538.75]	469.00 [291.00, 1121.50]	0.041
Age (Years)	/	54.25 ± 11.00	57.11 ± 12.63	0.305
Gender (%)	Female	13 (18.1)	3 (11.1)	0.596
	Male	59 (81.9)	24 (88.9)	
T (%)	T1	57 (79.2)	12 (44.4)	0.003
	T2	10 (13.9)	8 (29.6)	
	T3	5 (6.9)	5 (18.5)	
	T4	0 (0.0)	2 (7.4)	
N (%)	N0	66 (100.0)	24 (100.0)	NA
M (%)	M0	64 (100.0)	22 (95.7)	0.591
	M1	0 (0.0)	1 (4.3)	
TNM_stage (%)	Stage I	56 (78.9)	12 (46.2)	0.006
	Stage II	10 (14.1)	8 (30.8)	
	Stage III	5 (7.0)	5 (19.2)	
	Stage IV	0 (0.0)	1 (3.8)	
Grade (%)	G1	4 (5.6)	2 (7.4)	0.028
	G2	33 (45.8)	4 (14.8)	
	G3	30 (41.7)	16 (59.3)	
	G4	5 (6.9)	5 (18.5)	
Adjacent hepatic tissue inflammation extent type (%)	Mild	25 (50.0)	17 (81.0)	0.033
	None	20 (40.0)	2 (9.5)	
	Severe	5 (10.0)	2 (9.5)	
Child-Pugh (%)	A	65 (92.9)	25 (96.2)	0.771
	B	4 (5.7)	1 (3.8)	
	C	1 (1.4)	0 (0.0)	
Vascular invasion (%)	Macro	2 (2.8)	2 (8.0)	<0.001
	Micro	10 (14.1)	13 (52.0)	
	None	59 (83.1)	10 (40.0)	

Supplementary Table 2. Details of the ten models.

Journal	PMID	First Author	Gene	Coefficient
Journal of medical virology	37721443	Xinhao Peng	ACLY	0.007
Journal of medical virology	37721443	Xinhao Peng	SQSTM1	0.0009
Journal of medical virology	37721443	Xinhao Peng	RIPK2	0.025
Journal of medical virology	37721443	Xinhao Peng	S100A9	0.0002
Journal of medical virology	37721443	Xinhao Peng	NLRP4	0.1681
Clinical and Investigative Medicine	34600458	Jia Shen	DSCR4	0.3576
Clinical and Investigative Medicine	34600458	Jia Shen	DBH	0.3273
Clinical and Investigative Medicine	34600458	Jia Shen	ECM1	-0.8191
Clinical and Investigative Medicine	34600458	Jia Shen	GDAP1	0.6525
Clinical and Investigative Medicine	34600458	Jia Shen	MATR3	2.1210
Clinical and Investigative Medicine	34600458	Jia Shen	RFC4	0.0790
BMC Gastroenterology	37957550	Ping Yan	ACADVL	-0.5362
BMC Gastroenterology	37957550	Ping Yan	ACAT1	-0.3284
BMC Gastroenterology	37957550	Ping Yan	ACSL3	0.6345
BMC Gastroenterology	37957550	Ping Yan	ADH4	-0.1621
BMC Gastroenterology	37957550	Ping Yan	ECI1	-0.0467
Frontiers in Immunology	37180150	Jianming Dong	PINK1	-0.4025
Frontiers in Immunology	37180150	Jianming Dong	LGALS3	0.2081
Frontiers in Immunology	37180150	Jianming Dong	G6PD	0.2371
Infectious Agents and Cancer	36474267	Lei Wang	HMMR	0.142113311
Infectious Agents and Cancer	36474267	Lei Wang	MCM6	0.084558199
Infectious Agents and Cancer	36474267	Lei Wang	TPX2	0.285390199
Infectious Agents and Cancer	36474267	Lei Wang	KIF20A	0.08339874
Infectious Agents and Cancer	36474267	Lei Wang	CCL20	0.029641894
Infectious Agents and Cancer	36474267	Lei Wang	RGS2	0.031218559
Infectious Agents and Cancer	36474267	Lei Wang	NUSAP1	-0.449566369
Infectious Agents and Cancer	36474267	Lei Wang	FABP5	0.002614688
Infectious Agents and Cancer	36474267	Lei Wang	FZD6	0.017389305
Infectious Agents and Cancer	36474267	Lei Wang	PBK	0.094068871
Infectious Agents and Cancer	36474267	Lei Wang	STK39	0.032363425
Molecular Medicine	32552682	Qiongxuan Fang	HNRNPA2B1	0.0125
Molecular Medicine	32552682	Qiongxuan Fang	RBM15	0.5117
Journal of Oncology	36072970	Zhenfu Gao	ATIC	0.015
Journal of Oncology	36072970	Zhenfu Gao	KIF2C	0.0417
Journal of Cancer	31737106	Xiwen Liao	TOP2A	0.628
Journal of Cancer	31737106	Xiwen Liao	PRC1	0.231
Frontiers in Immunology	38799437	Jinyue Tian	CHMP4C	NA
Frontiers in Immunology	38799437	Jinyue Tian	DLAT	NA
Frontiers in Immunology	38799437	Jinyue Tian	MMP1	NA
Frontiers in Immunology	38799437	Jinyue Tian	NLRP6	NA

Frontiers in Immunology	38799437	Jinyue Tian	NOD2	NA
Frontiers in Genetics	34539726	Jingyuan Zhang	PTTG1	NA
Frontiers in Genetics	34539726	Jingyuan Zhang	MAD2L1	NA
Frontiers in Genetics	34539726	Jingyuan Zhang	PCLAF	NA
Frontiers in Genetics	34539726	Jingyuan Zhang	RRM2	NA
Frontiers in Genetics	34539726	Jingyuan Zhang	TPX2	NA
Frontiers in Genetics	34539726	Jingyuan Zhang	CDK1	NA
Frontiers in Genetics	34539726	Jingyuan Zhang	NEK2	NA
Frontiers in Genetics	34539726	Jingyuan Zhang	DEPDC1	NA
Frontiers in Genetics	34539726	Jingyuan Zhang	ZWINT	NA

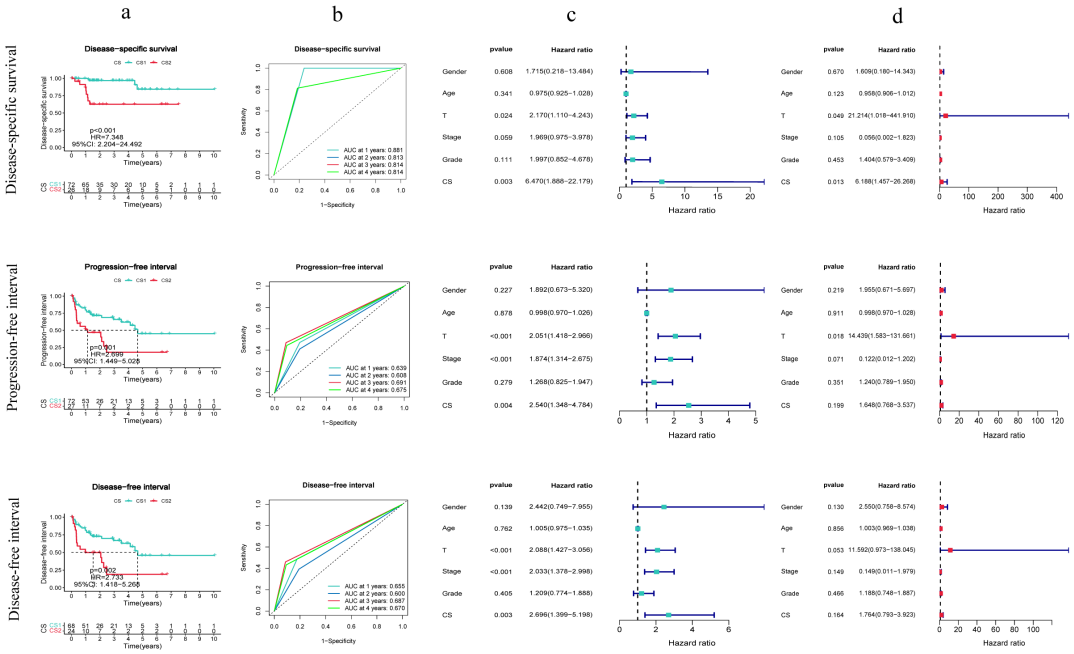

Supplementary Figure 1. Effects of CS on DSS, PFI, and DFI of HBV-HCC in the TCGA-LIHC cohort. a KM curves revealing differences in DSS, PFI, and DFI between HBV-HCC in CS1 and CS2 groups. **b** ROC curves reveal the ability of CSs to predict DSS, PFI, and DFI in HBV-HCC. **c-d** Univariate and multivariate Cox regression analyses revealing the effect of CSs on HBV-HCC patients' DSS, PFI, and DFI.

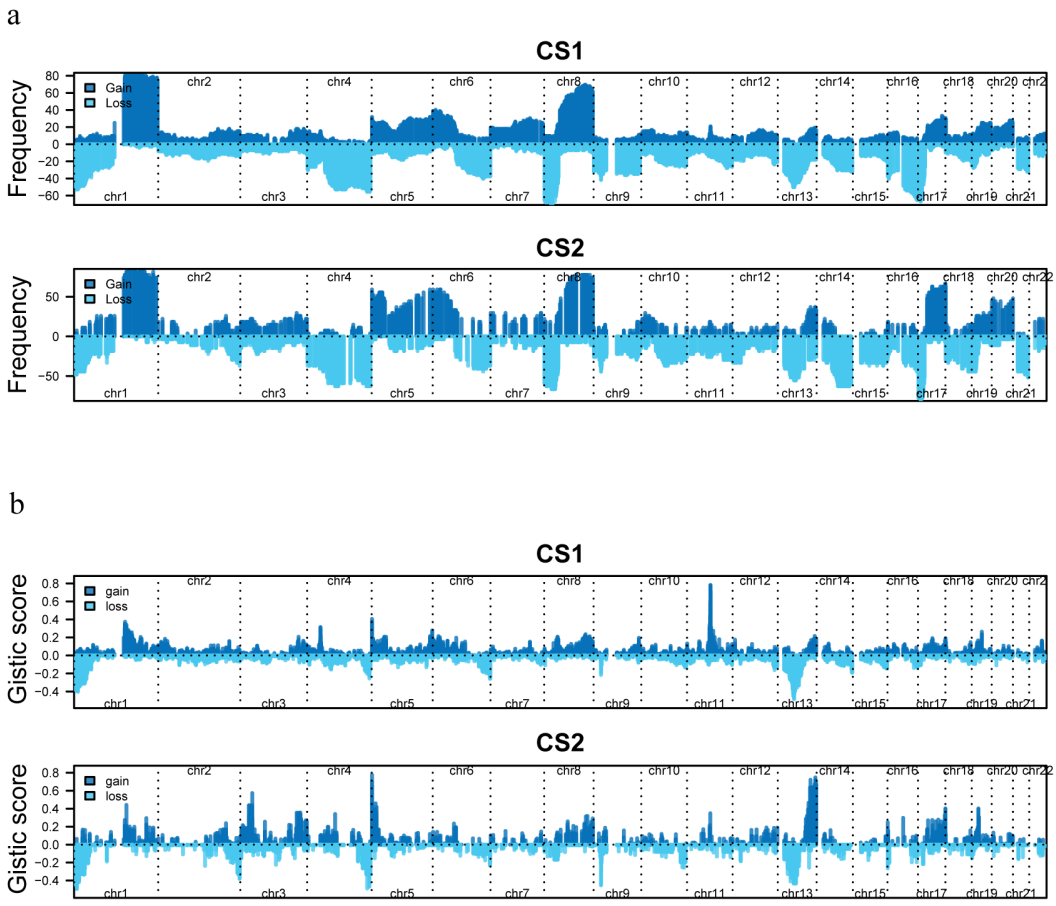

Supplementary Figure 2. Differences in CNV frequency and gistic scores between patients with different CSs. a CNV frequency; **b** gistic scores.

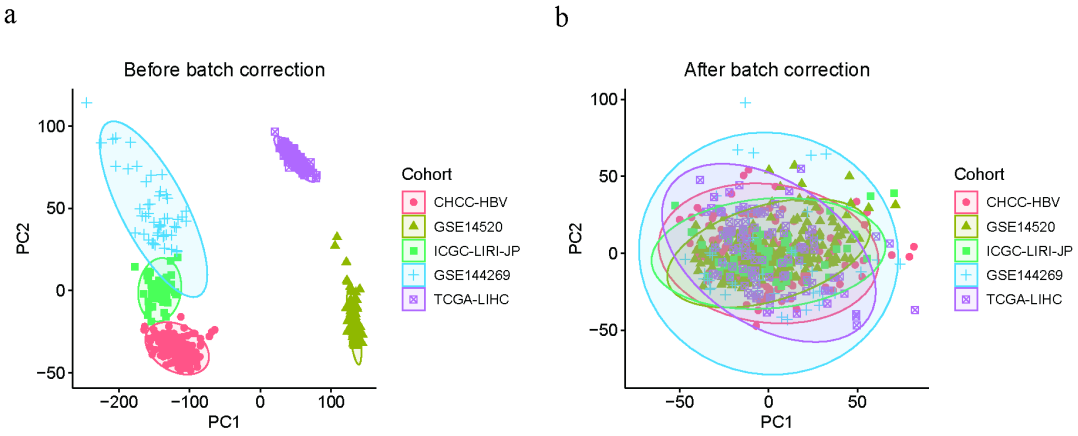

Supplementary Figure 3. Principal component analysis results of five cohorts before and after batch effect correction (a: before; b: after)

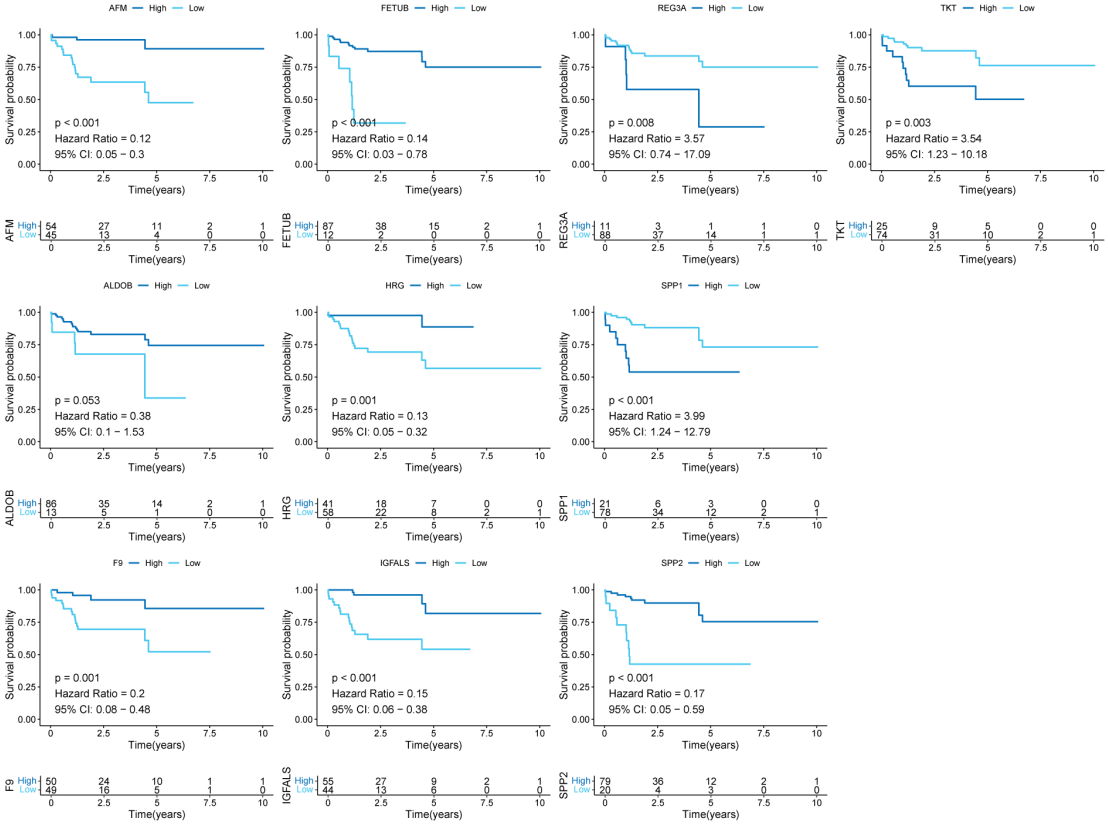

Supplementary Figure 4. Effects of the ten genes included in the algorithmic combination of RSF+Enet[alpha=0.2] on OS in HBV-HCC patients in TCGA-LIHC cohort.

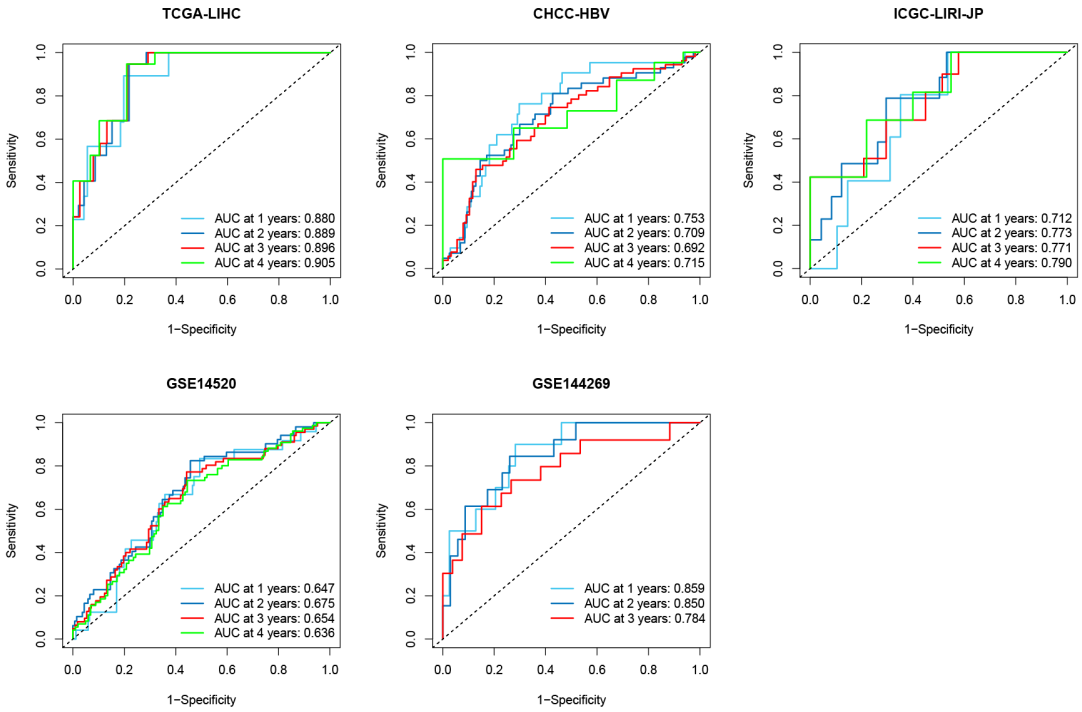

Supplementary Figure 5. ROC curves reveal the ability of MLPS to predict OS in HBV-HCC in the five cohorts.

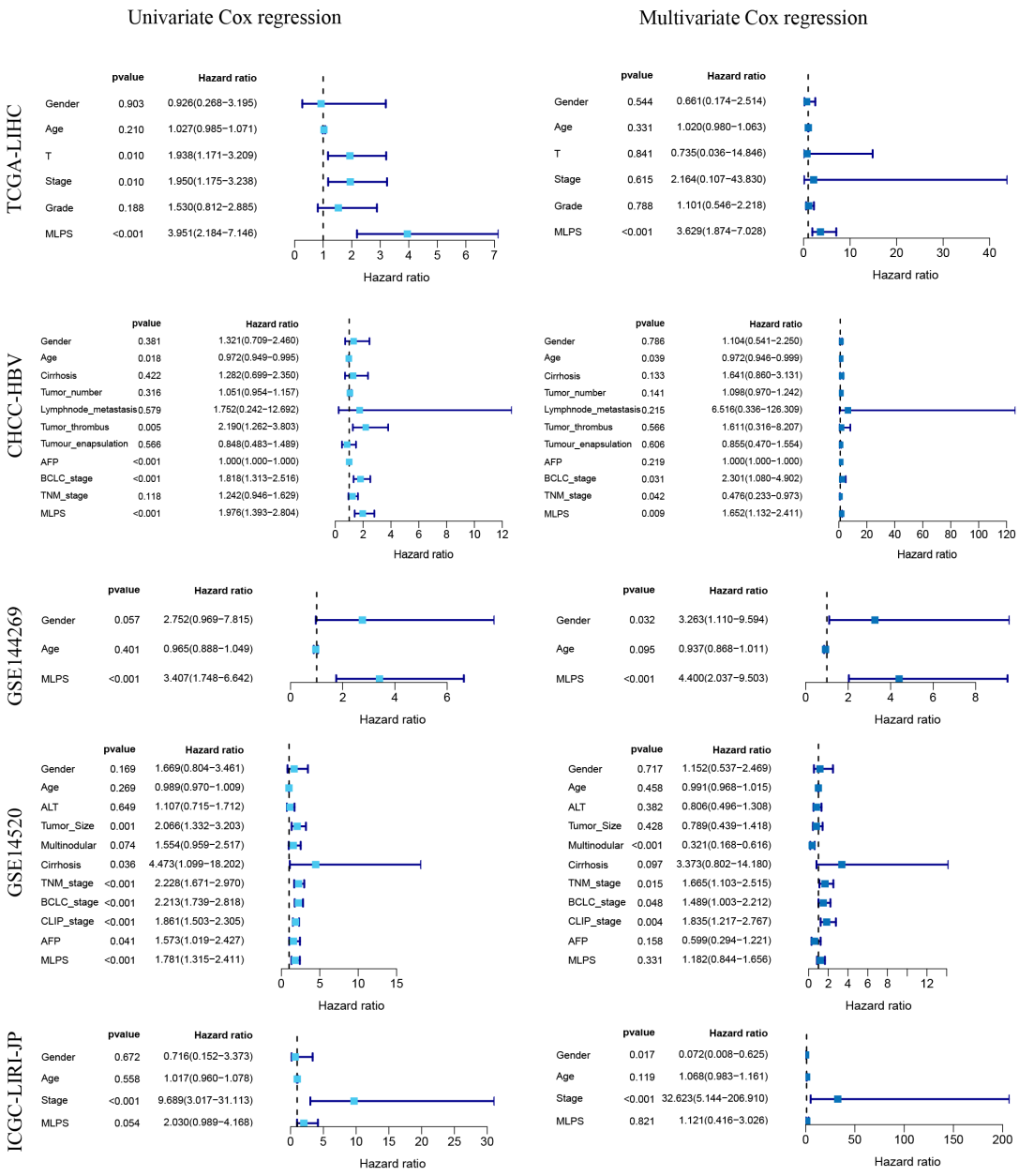

Supplementary Figure 6. Univariate and multivariate Cox regression analyses revealing the effect of MLPS on OS in the five cohorts.

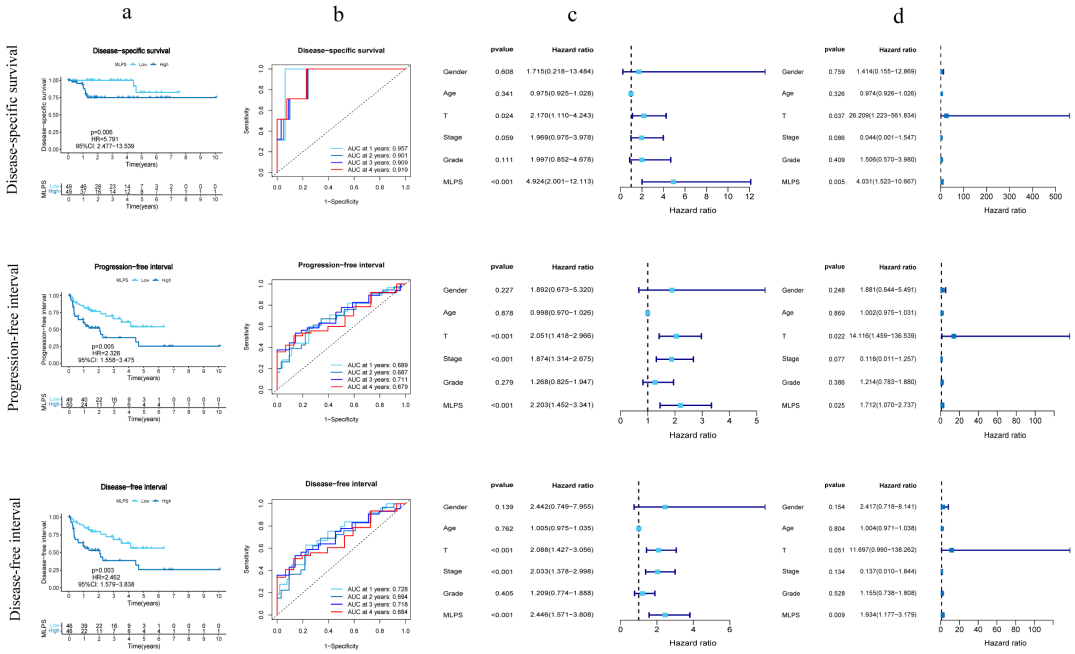

Supplementary Figure 7. Effects of MLPS on HBV-HCC in TCGA-LIHC cohort. a Differences in DSS, PFI, and DFI between HBV-HCC patients in the high-MLPS and low-MLPS groups. **b** ROC curves reveal the ability of MLPS to predict DSS, PFI, and DFI in HBV-HCC. **c-d** Univariate and multivariate Cox regression analyses revealing the effect of MLPS on HBV-HCC patients' DSS, PFI, and DFI.

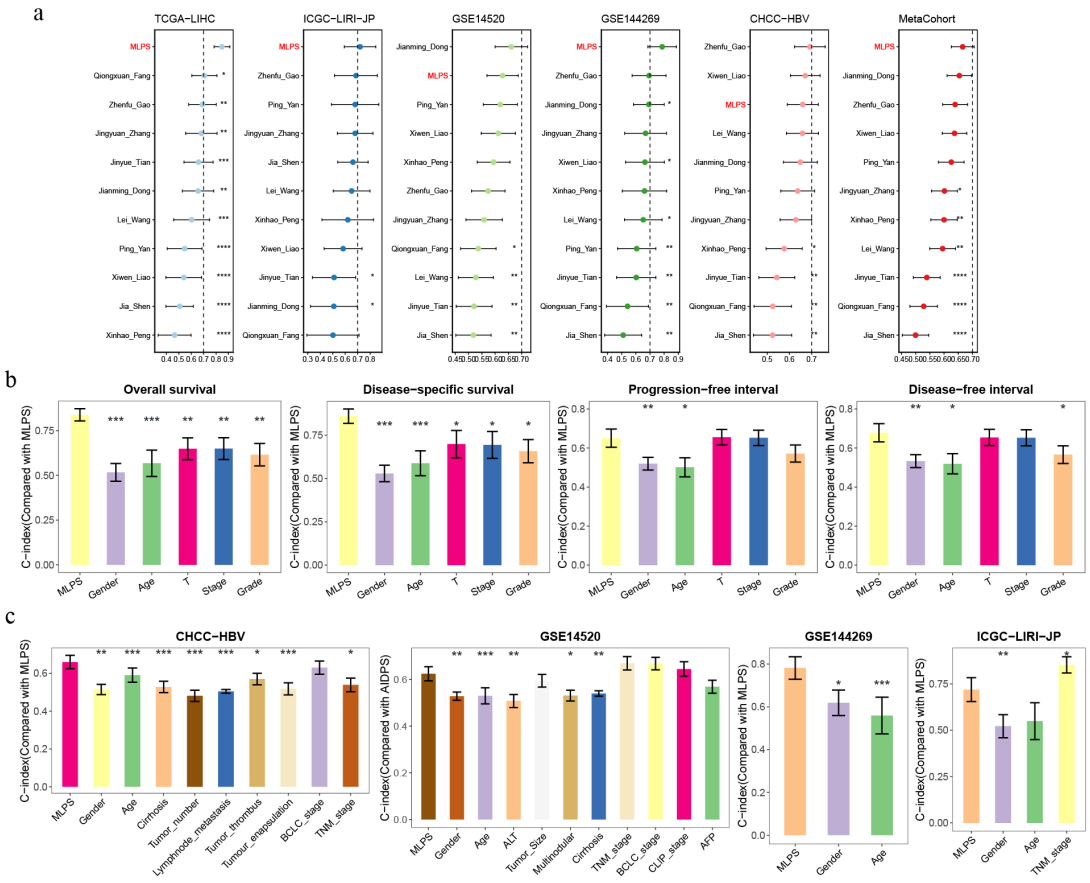

Supplementary Figure 8. Superiority and robustness of MLPS in predicting prognosis of HBV-HCC. a C-index of MLPS compared with ten models on prognosis of HBV-HCC patients. **b** Comparison of the C-index of OS, DSS, PFI, and DFI in the TCGA-LIHC cohort of patients with MLPS and other clinical characteristics prognostic of HBV-HCC. **c** Comparison of C-index of OS in MLPS with other clinical characteristics of prognostic HBV-HCC patients in GSE14520, GSE144269, ICGC-LIRI-JP, and CHCC-HBV cohorts.

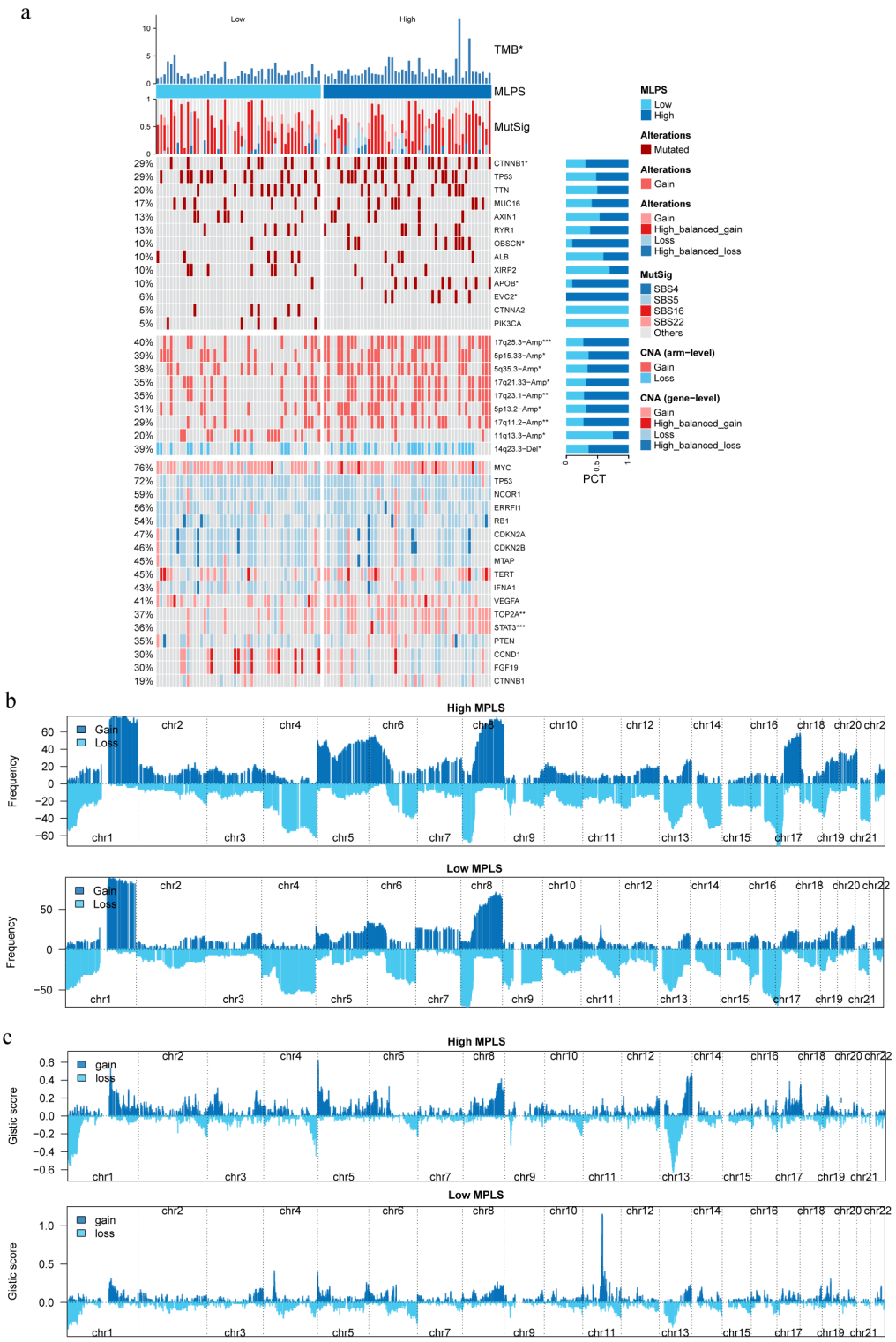

Supplementary Figure 9. Differences in genomic variation between high-MLPS and low-MLPS scores HBV-HCC patients. a ComplexHeatmap revealing genomic variation among different MLPS group. Differences in CNV frequency and gistic scores between patients with different MLPS groups (**b** CNV frequency. **c** gistic scores).

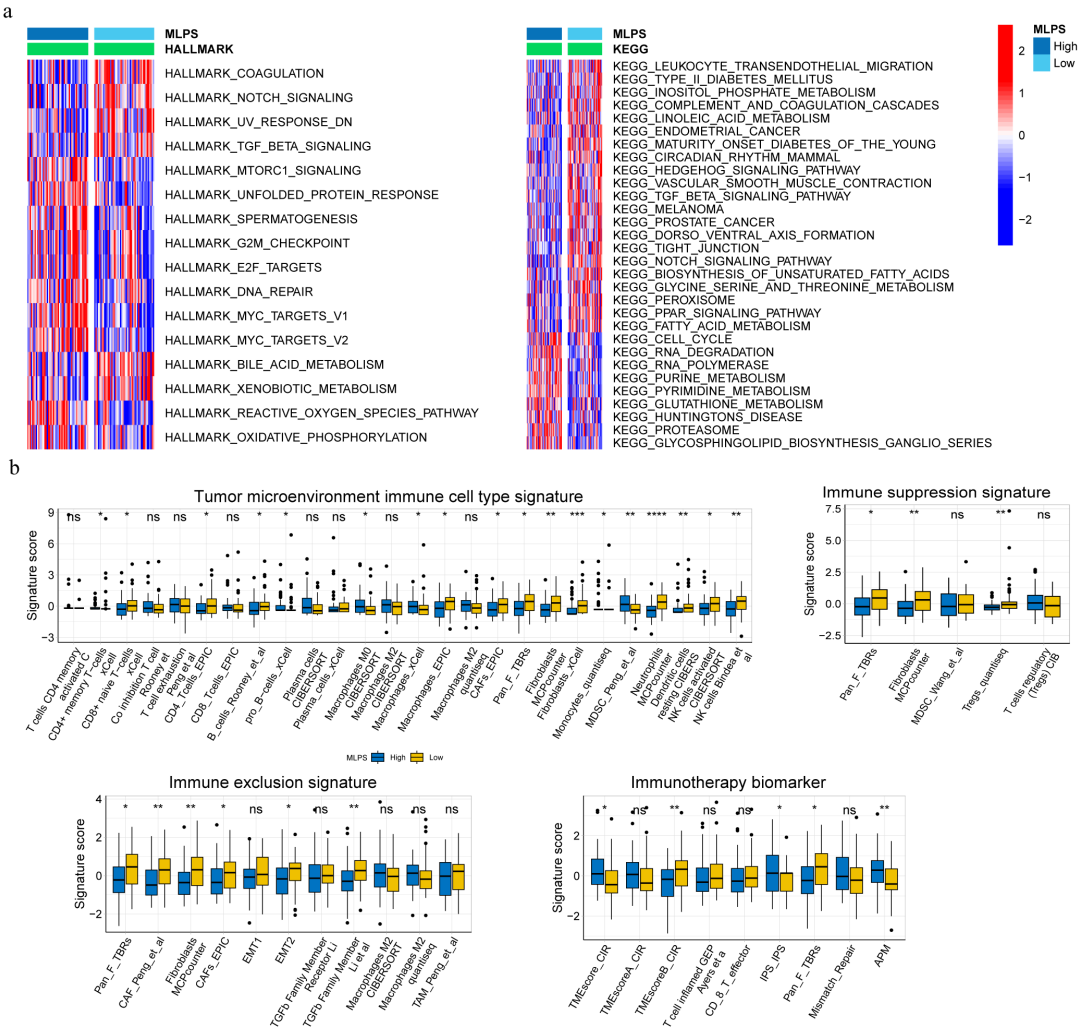

Supplementary Figure 10. Differences in biological function and immune landscape between high-MLPS and low-MLPS scores HBV-HCC patients. a Functional difference between different HBV-HCC MLPS group based on KEGG and hallmark terms. **b** Differences in the immune landscape between HBV-HCC MLPS groups.

Supplementary Figure 11. Uncropped and unprocessed scan of blots.